Heliyon 10 (2024) e27466

Contents lists available at ScienceDirect

Heliyon

journal homepage: www.cell.com/heliyon

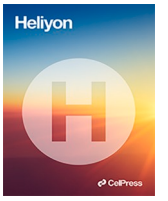

Research article

CDKN1A regulation on chondrogenic differentiation of human chondrocytes in osteoarthritis through single-cell and bulk sequencing analysis

Chao Fang [a,1], Shanbang Zhu [b,1], Rui Zhong [a,1], Gang Yu [a], Shuai Lu [a], Zhilin Liu [a], Jingyu Gao [a], Chengyuan Yan [a], Yingming Wang [a], Xinzhe Feng [c,*]

[a] *Department of Orthopedics, The First Affiliated Hospital of USTC, Hefei, 230001, China*
[b] *Department of Orthopedics, Affiliated Jinling Hospital, Medical School of Nanjing University, No 305 Zhongshandonglu Road, Nanjing, 210002, China*
[c] *Department of Joint Bone Disease Surgery, Changhai Hospital, Naval Medical University, Shanghai, 200433, China*

ARTICLE INFO

Keywords:
Programmed cell death related genes
Osteoarthritis (OA)
Principal component analysis (PCA)
T-distributed stochastic neighbor embedding (t-SNE)
Weighted gene co-expression network analysis (WGCNA)
Least absolute shrinkage and selection operator (LASSO)
Boruta algorithm

ABSTRACT

Objective: Chondrocyte death is the hallmark of cartilage degeneration during osteoarthritis (OA). However, the specific pathogenesis of cell death in OA chondrocytes has not been elucidated. This study aims to validate the role of CDKN1A, a key programmed cell death (PCD)-related gene, in chondrogenic differentiation using a combination of single-cell and bulk sequencing approaches.
Design: OA-related RNA-seq data (GSE114007, GSE55235, GSE152805) were downloaded from Gene Expression Omnibus database. PCD-related genes were obtained from GeneCards database. RNA-seq was performed to annotate the cell types in OA and control samples. Differentially expressed genes (DEGs) among those cell types (scRNA-DEGs) were screened. A nomogram of OA was constructed based on the featured genes, and potential drugs targeting the featured genes were predicted. The presence of key genes was confirmed using Real-Time Quantitative Polymerase Chain Reaction (RT-qPCR), Western blot (WB), and immunohistochemistry (IHC). Micromass culture and Alcian blue staining were used to determine the effect of CDKN1A on chondrogenesis.
Results: Six cell types, namely HomC, HTC, RepC, preFC, FC, and RegC, were annotated in scRNA-seq data. Five featured genes (*JUN, CDKN1A, HMGB2, DDIT3,* and *DDIT4)* were screened by multiple biological information analysis methods. TAXOTERE had the highest ability to dock with DDIT3. Functional analysis indicated that CDKN1A was enriched in processes related to collagen catabolism and acts as a positive regulator of autophagy. Additionally, CDKN1A was found to be associated with several KEGG pathways, including those involved in acute myeloid leukemia and autoimmune thyroid disease. CDKN1A was confirmed down-regulated in the joint tissues of OA mouse model and OA model cell. Inhibiting the expression of CDKN1A can significantly suppress the differentiation of OA chondrocytes.
Conclusion: Our findings highlight the critical role of CDKN1A in promoting cartilage formation in both *in vivo* and *in vitro* and suggest its potential as a therapeutic target for OA treatment.

* Corresponding author. Department of Joint Bone Disease Surgery, Changhai Hospital, Naval Medical University, Shanghai, 200433, China.
E-mail address: fengxinzheazxc@smmu.edu.cn (X. Feng).
[1] These authors contributed equally to this work.

https://doi.org/10.1016/j.heliyon.2024.e27466
Received 10 October 2023; Received in revised form 28 February 2024; Accepted 29 February 2024
Available online 4 March 2024

1. Introduction

Osteoarthritis (OA) is a chronic and degenerative disorder of the entire joint and a major cause of joint pain and disability [1]. An imbalance in joint homeostasis is caused by multiple factors, including trauma, mechanical instability, inflammation, aging, obesity, and heredity [2], all of which eventually result in articular cartilage damage, subchondral bone marrow cysts, synovial hyperplasia, and osteophyte formation [3]. Currently, OA is the most common joint disease affecting more than 240 million people worldwide [4]. Unfortunately, neither pharmacological intervention nor surgical treatment can completely reverse cartilage lesions. Oral medications are the primary treatments for patients with early-stage OA. However, these treatments have obvious side effects and can only be administered in small doses [5]. Although joint replacement can achieve a clinical curative effect in patients with advanced OA, operational safety cannot be guaranteed [6]. Emerging OA therapeutic approaches include stem cells, protease inhibitors, and bone biomaterials. These new measures are effective in basic research; however, they exhibit low clinical credibility [7]. Therefore, there is an urgent need to investigate the pathogenesis of OA and search for gene-targeted therapies.

As the only cell type in the cartilage, chondrocytes undergo elevated synthetic activity during the initial stages of OA [8]. During OA progression, senescent chondrocytes increase in number and produce degradative enzymes (ADAMTS-5 and MMP-13) and inflammatory mediators (IL-1β, TNF-α, and IL-6). This disrupts the balance between cartilage synthesis and degradation, leading to proteoglycan depletion and erosion of the collagen network [9]. Finally, chondrocyte death occurs [10].Programmed cell death (PCD) is a basic biological process that regulates homeostasis and is crucial for growth and development. Cartilage loss mediated by chondrocyte PCD is a key mechanism in the pathogenesis of OA [11]. OA-associated chondrocyte death primarily involves five classical pathways: apoptosis, necrosis, pyroptosis, ferroptosis, and autophagy [12]. However, little is known about the chondrocyte subsets present in OA cartilage. The developmental trajectory and functional expression of cell subsets related to OA progression and the mutual regulatory relationships among cell subsets remain ambiguous, ultimately hindering our understanding of the OA development.

Single-cell RNA sequencing (scRNA-seq) can be used to breakdown human tissues into single cells and cell subgroups and can recognize different cell subgroups in tissues at the resolution level of a single cell [13]. An independent analysis was previously performed to reveal the relationship between cell subsets and the process of gene interrelation within cells [14]. However, the use of RNA-Seq in OA research is still in its initial stages, and few studies have used RNA-seq to investigate the molecular characteristics of OA. Therefore, we conducted comprehensive scRNA-seq and bulk sequencing to identify the expression patterns of programmed PCD genes in osteoarthritic chondrocytes.

In this study, six chondrocyte subtypes were identified using scRNA-seq. Of these subtypes, only the HomC subtype significantly differed between the normal and OA groups. In fact, the expression of the HomC subtype was downregulated in the OA group. The DEGs in the HomC subtype intersected with the classical PCD gene set, and cyclin-dependent kinase inhibitor-1A (CDKN1A) was targeted through confirmatory tests *in vitro* and *in vivo*. CDKN1A was demonstrated to influence the progression of chondrocyte death by regulating the HomC subtype. Using a combination of bioinformatics approaches based on different types of data (single-cell RNA-seq and bulk RNA-seq) and multilevel experimental verification, we aimed to elucidate the role of key genes related to PCD in OA and provide a theoretical foundation for targeted OA therapy.

2. Materials and methods

2.1. Data collection

OA-related RNA-seq data (all OA types) were downloaded from the Gene Expression Omnibus (GEO) database (https://www.ncbi.nlm.nih.gov/geo/). The RNA-seq data in GSE114007, including 18 control and 20 OA samples, were used as the training set; the RNA-seq data in GSE55235, which comprised 10 control and 10 OA samples, were used as the validation set; and the scRNA-seq data in GSE152805, including three control and three OA samples, were employed for single-cell analyses. A total of 616 PCD-related genes were obtained from the GeneCards database (https://www.genecards.org/).

2.2. Single-cell RNA-seq analysis of GSE152805

The scRNA-seq data in GSE152805 were analyzed using the "Seurat" package (version 4.1.0). First, genes that were detected in fewer than three cells, cells with fewer than 200 detected genes, and cells with more than 7500 detected genes were eliminated, and the mitochondrial gene expression proportion was limited to less than 5% to obtain high-quality cells. The top 2000 genes with the highest expression differences among the high-quality cells were selected for further analysis. Principal component analysis (PCA) was then applied to rule out outlier cells and obtain the principal components (PCs). A T-distributed stochastic neighbor embedding (t-SNE) algorithm was used to cluster the PCs. Subsequently, marker genes in each cluster were identified, and the differences in the expression of marker genes between clusters were compared using the Wilcoxon test. Marker genes that were differentially expressed were visualized via a heatmap and a scatter plot using the "gglot2" package (version 3.3.5) and "pheatmap" package (version 1.0.12) [15]. Clusters were manually annotated based on the marker genes of the chondrocyte subtypes obtained from a previous study [16]. The expression levels of these marker genes were observed in all cells. DEGs among the different cell types (scRNA-DEGs) were identified using the "FindMarkers" method with *adj.* $p < 0.05$ and $|\log_2 FC| > 0.5$. Finally, a pseudotime trajectory analysis of these cell types was performed.

2.3. Differential analysis and weighted gene coexpression network analysis (WGCNA) of OA

DEGs between OA and control samples in GSE114007 were identified using the "limma" package (version 3.48.3) with $|\log_2 FC| > 1$ and *adj.* $p < 0.05$ [17]. WGCNA was conducted using the "WGCNA" package (version 1.70–3) to obtain coexpression modules and hub genes related to OA [18]. The samples were clustered to detect outliers, and a suitable soft threshold (β) was selected based on the scale-free topology fit. Genes were then allocated to different coexpression modules using a dynamic tree-cutting algorithm based on β. The modules were merged according to their cut heights. The module with the highest degree of correlation with OA was selected, and the genes in the module were defined as hub genes for further analysis.

2.4. Screening of the featured OA-related genes using machine learning algorithms

Hub genes were compared with the DEGs between OA and control samples, scRNA-DEGs, and PCD-related genes to identify candidate genes. The "clusterProfiler" package (version 4.0.2) was used to identify the enriched Gene Ontology (GO) functions and Kyoto Encyclopedia of Genes and Genomes (KEGG) pathways of the genes according to $p < 0.05$ and count ≥ 1 [19]. Candidate genes were then filtered using the Boruta algorithm and least absolute shrinkage and selection operator (LASSO) algorithm. The featured genes were obtained by overlapping the genes screened by the above algorithms. Receiver operating characteristic (ROC) analysis was performed to verify the predictive performance of these genes. Thereafter, the expression levels of the featured genes were compared between the control and OA samples in the training and validation sets.

2.5. Construction of a nomogram based on the featured genes

Gene set enrichment analysis (GSEA) was conducted using the "ClusterProfiler" package to identify the enriched GO functions and KEGG pathways of each featured gene according to $|NES| > 1$, NOM $p < 0.05$, and $q < 0.25$. Thereafter, a nomogram of OA was generated using the "rms" package (version 6.1–0) based on the featured genes. Correction, DCA, and clinical impact curves were constructed to verify the predictive performance of the nomogram.

2.6. Drug prediction and molecular docking

Potential drugs targeting the featured genes were predicted using the DGIdb database, and a drug–gene network was constructed (https://dgidb.genome.wustl.edu/). Subsequently, the PDB files of proteins related to the featured genes were downloaded from the RCSB database (https://www1.rcsb.org/), and the SDF files of potential drugs were obtained from the DrugBank database (https://go.drugbank.com/). AutoDock was used to detect and visualize the molecular docking conditions between the drugs and featured genes.

2.7. Chondrocyte culture

C28/I2 human chondrocytes were cultured in Dulbecco's modified Eagle's medium (DMEM) supplemented with 10% fetal bovine serum (FBS) and 1% penicillin and streptomycin. The medium was changed every 2 days. The *in vitro* OA model was induced via treatment with interleukin-1β (IL-1β, 20 ng/m) for 3 days.

2.8. Micromass culture and alcian blue staining

C28/I2 human chondrocytes were resuspended at a density of 2.0×10^7 cells/mL. Micromass cultures of cells were suspended in the center of a 24-well plate and incubated at 37 °C with 5% CO_2. Chondrogenic induction was performed for 1, 7, and 14 days. Thereafter, alcian blue staining was performed according to the manufacturer's instructions [20]. Images were captured at room temperature using a high-resolution camera (EOS 850D; Canon).

2.9. CDKN1A-knockout C28/I2 human chondrocyte cell lines

The CDKN1A CRISPR/Cas9 KO plasmid (#sc-400013) and CDKN1A homology-directed repair (HDR) plasmid (#sc-400013-HDR) (Santa Cruz Biotechnology) were transfected into C28/I2 human chondrocytes using Lipofectamine 3000 (Invitrogen).

2.10. OA mouse model

All surgical procedures were approved by the standards and guidelines of the Bioethics Committee of The First Affiliated Hospital of the University of Science and Technology of China. To establish the OA model, the medial meniscus (DMM) in the right limb of 10-week-old C57BL/6 male mice was destabilized, as previously described [21]. Mice were randomly assigned to two groups (n = 8): control (opening the knee capsule before stitching) and OA (DMM model). All mice were sacrificed, and the joints were harvested 8 weeks after the operation [22].

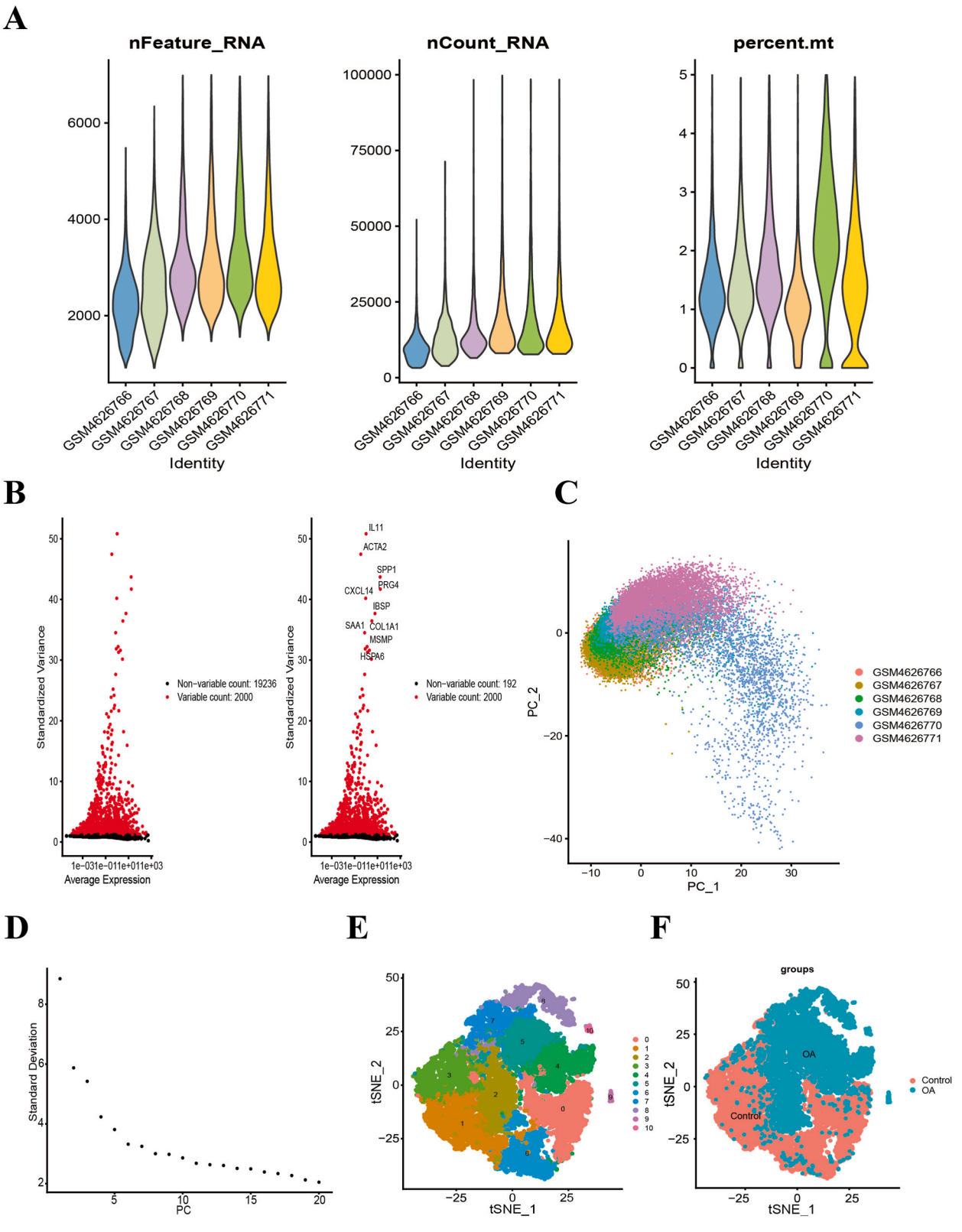

(caption on next page)

Fig. 1. Quality control and cell type identification of the single-cell dataset GSE152805. (A) Basic information of the dataset displayed by violin plots. nFeature RNA: the number of genes detected in each cell; nCount: the sum of the expression of all genes detected in each cell; percent. mt: the proportion of mitochondrial genes detected in each cell. (B) Identification of highly variable genes. Red: highly variable genes; Black: non-highly variable genes. (C) (D) Principal component analysis. The distribution of cells in different samples and standard deviation of the cell clusters. (E) The top 20 PCs were subjected to clustering analysis using the t-SNE algorithm. The resulting clusters were then co-clustered into 11 distinct cellular taxa, representing different cell types (F) Distribution of different cell taxa in OA and control. t-SNE: t-distributed stochastic neighbor embedding, Blue represents the OA group, and red represents the Control group. (For interpretation of the references to color in this figure legend, the reader is referred to the Web version of this article.)

2.11. Real-time qPCR

The micromass cells were harvested for RT–qPCR. Total RNA extraction, cDNA synthesis, and RT–qPCR was performed as previously described [20]. The primers used for sequencing are listed in Supplemental Table 6.

2.12. Western blot

Cell lysates were separated using sodium dodecyl sulfate–polyacrylamide gel electrophoresis and transferred onto nitrocellulose membranes. The membrane was then blocked with TBST in 5% skim milk for 1 h (room temperature) and incubated with the primary antibodies overnight (4 °C) followed by the secondary antibody for 1 h (room temperature). The results were visualized using a chemiluminescence system (Bio-Rad).

2.13. Safranin O and immunochemistry staining

The knee joints of mice were fixed in 4% PFA for 48 h and decalcified in 10% EDTA for 2 weeks. Safranin O and immunochemical staining were performed as previously described [23]. Antibodies against CDKN1A (ab102013) and JUN (ab102013) were purchased from Abcam (Cambridge, UK). The number of positively stained cells in the cartilage was quantified using ImageJ software.

3. Results

3.1. scRNA-seq analysis of OA

A total of 25,808 high-quality cells were screened based on quality control by eliminating ineligible genes and cells (Fig. 1A), and the top 2000 genes with the highest degree of expression difference among the high-quality cells were obtained (Fig. 1B). Based on PCA, no outlier samples needed to be eliminated, and the cells were divided into 20 PCs (Fig. 1C and D). The 20 PCs were then analyzed using the t-SNE algorithm to divide them into 11 clusters. Notably, OA cells were mainly concentrated in Clusters 2, 4, 5, 7, and 8 (Fig. 1E and F). Marker genes were then obtained from each cluster with a high degree of difference, such as TNFRSF11B and *COMP*, and visualized on a heatmap (Fig. 2A). Based on the marker genes of the chondrocyte subtypes, the clusters were manually annotated into 6 cell types, including HomC, HTC, RepC, preFC, FC, and RegC (Fig. 2B) (Table S1). By observing the expression of those marker genes in cells, *COMP*, *OGN, CILP*, and *COL2A1* were found to be expressed in most cells (Fig. 2C). In addition, 735 scRNA DEGs were identified, and FC, RepC, and preFC were mainly transferred from HTC to HomCs (Fig. 2D and E).

3.2. Screening of 1987 DEGs and 2722 hub genes

A total of 1987 DEGs were identified between the OA and control samples using differential analysis (Fig. 3A and B) (Table S2). Sample clustering by WGCNA revealed that no outlier samples needed to be excluded (Fig. 3C). Genes were allocated to 11 coexpression modules by selecting $\beta = 6$, and these modules were further merged into seven modules according to the cut height of 0.3 (Fig. 3D–F). MEblack (n = 1923) and MEmagenta (n = 799), which had the highest positive and negative correlations with OA, respectively, were selected, and 2722 genes in the two modules were identified as hub genes for further analysis (Fig. 3G and H).

3.3. Screening of 5 featured genes using machine learning algorithms

A total of 13 candidate genes (*JUN, CDKN1A, HMGB2, ATF3, CTSC, ICAM1, NGF, DDIT3, DDIT4, PPP1R15A, HERPUD1, BNIP3*, and *NR4A2*) were identified by comparing the DEGs, scRNA-DEGs, PCD-related genes, and hub genes (Fig. 4A). Enrichment analysis revealed that the candidate genes were enriched in 481 GO functions, including the regulation of apoptosis and transcription regulator complex (Fig. 4B) (Table S3), and 30 KEGG pathways, including those related to apoptosis, lipid metabolism, and atherosclerosis (Fig. 4C) (Table S4). Thirteen genes screened by the Boruta algorithm and five genes screened by the LASSO algorithm were identified (Fig. 4D–F). Five featured genes, including *JUN, CDKN1A, HMGB2, DDIT3*, and *DDIT4*, were identified by comparing the two gene sets. The ROC curves demonstrated that all area under the curve (AUC) values were greater than 0.95 for the training (GSE114007) and validation (GSE55235) sets (Fig. 4G and H). The expression levels of all featured genes were significantly different between the OA and control samples. Notably, their trends in the two datasets were the same (Fig. 4I and J).

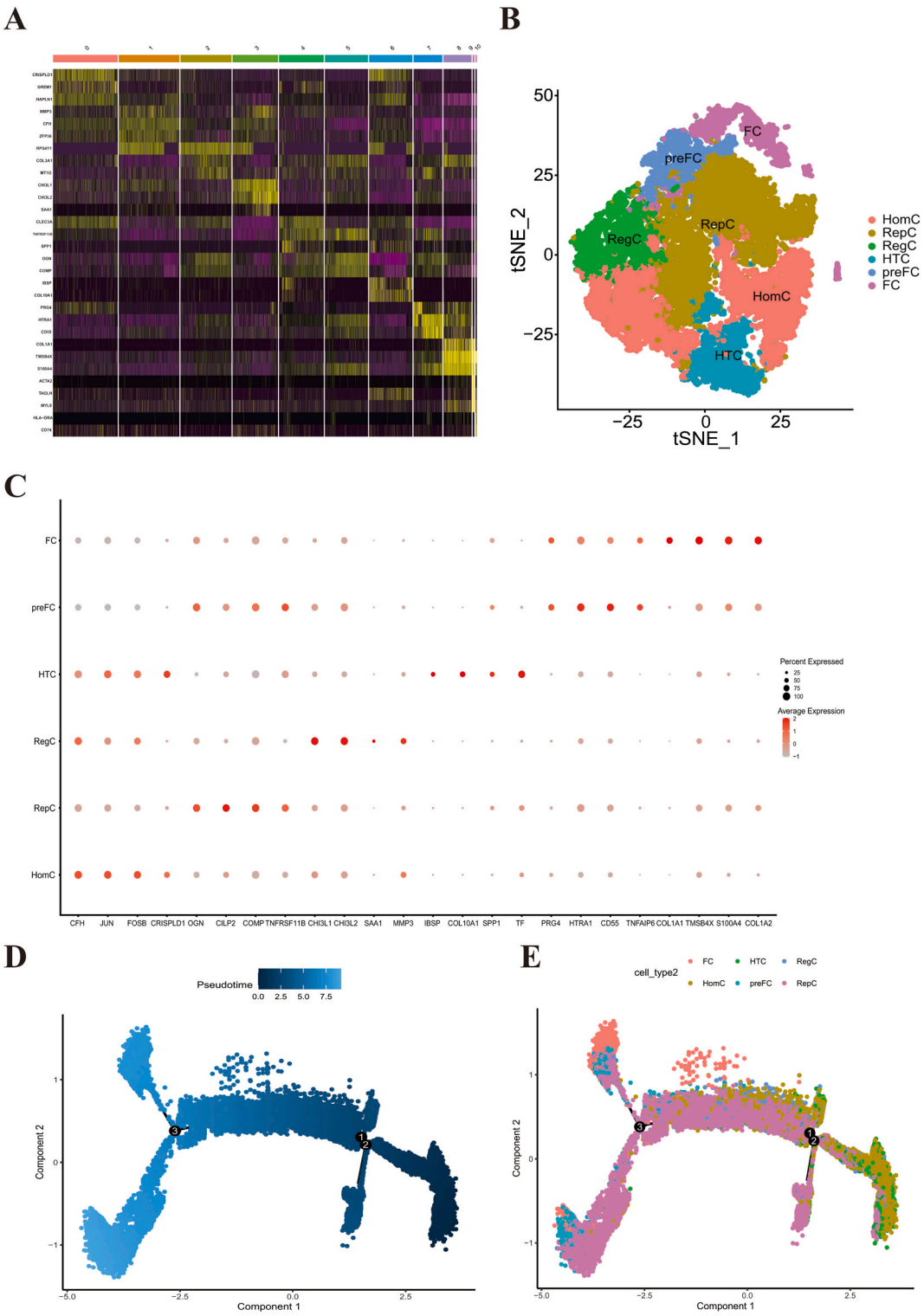

Fig. 2. Single-cell characterization and marker genes of the cell clusters and monocle pseudo-time analysis. (A) Marker genes of the cell clusters ae displayed via heat maps. (B) All 6 cell clusters in OA were annotated with singleR and CellMarker according to the composition of marker genes, namely HomC, HTC, RepC, preFC, FC, and RegC. (C) Expression of marker genes in the chondrocyte subtypes is displayed as bubble plots. (D) Pseudotime trajectory analysis of chondrocyte subtypes. The lighter the color, the closer the differentiation time. (E) Chondrocyte subtypes are labeled by colors in (D). (For interpretation of the references to color in this figure legend, the reader is referred to the Web version of this article.)

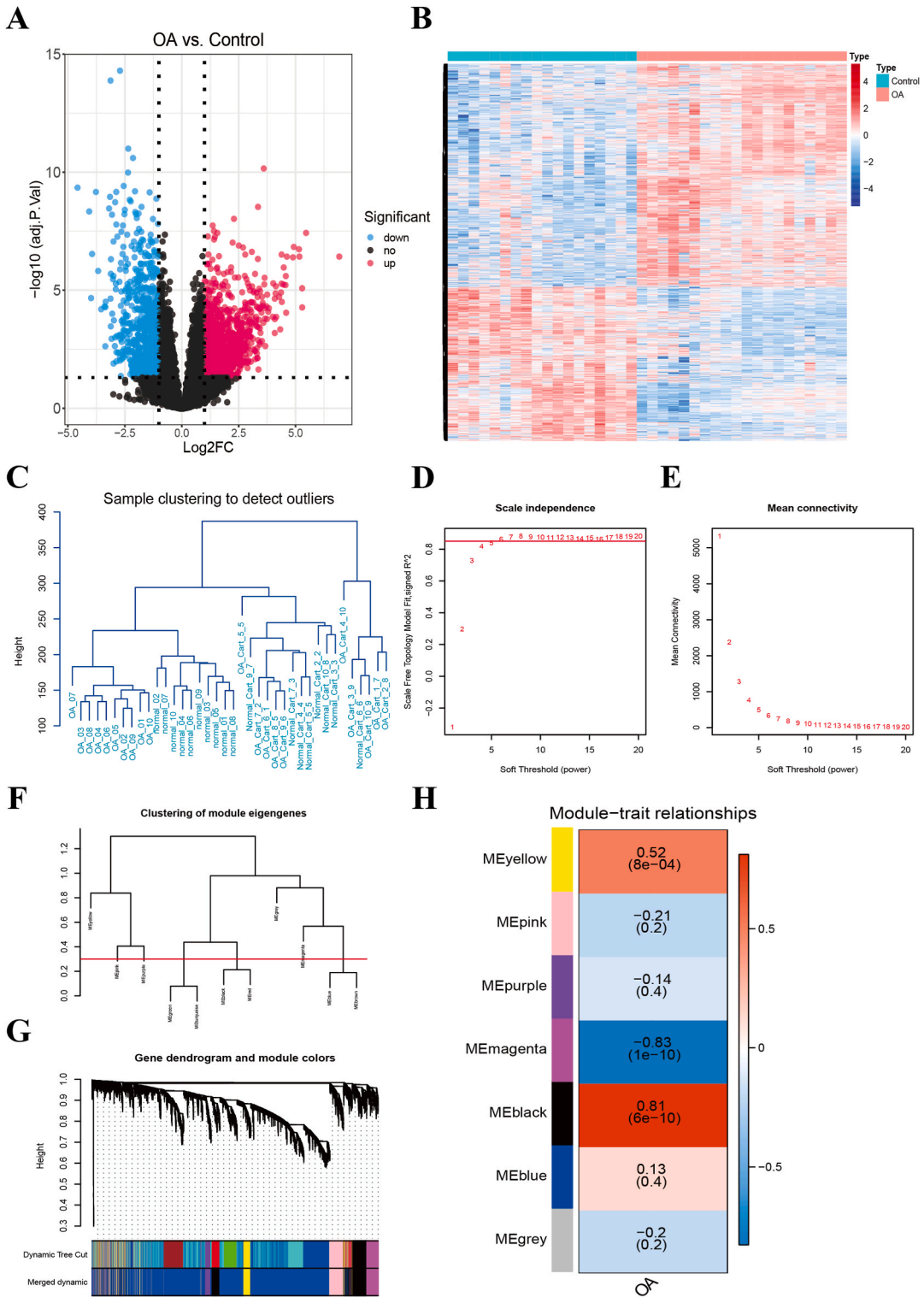

Fig. 3. Detection of DEGs between OA and control samples and identification of module genes of OA using WGCNA. (A) Volcano map of 1987 DEGs, including 1175 upregulated (red dots) and 812 downregulated genes (blue dots), between OA and control samples. (B) Heatmap of the expression of DEGs between OA and control samples. (C) Cluster analysis of samples for the detection of outliers. (D–E) The soft-thresholding power was selected based on the scale-free topology criterion, which measured the fit of the network to a scale-free distribution. The left panel showed the scale-free topology fit index (y-axis) plotted against different soft-thresholding powers (x-axis). The optimal soft-thresholding power was chosen as the lowest value that yields a scale-free topology fit index of 0.8. (F) Hierarchical clustering algorithm was used to group genes based on the

dissimilarity measurement (1-TOM). The dendrogram displayed the clustering results for all genes in the dataset. (G) Color band shows the results obtained from the automatic single-block analysis. Each branch represents one gene, and every color represents one co-expressed module. (H) Heat maps of the correlation between the modules and OA. Each row indicates a module eigengene (the first principal component of the gene expression matrix in a module). DEGs: Differentially expressed genes; TOM: topological overlap matrix. (For interpretation of the references to color in this figure legend, the reader is referred to the Web version of this article.)

3.4. Enrichment analysis and nomogram construction based on the featured genes

GSEA was performed to identify the enriched GO functions and KEGG pathways of each featured gene. These results provided clues for an in-depth understanding of the functions of the featured genes and the biological processes they were involved in, help to unravel the mechanisms of their roles in related diseases and physiological phenomena, and provided directions and potential therapeutic targets for future studies. In terms of GO functions, *JUN* was found to be enriched in chromosome segregation and external encapsulating structural organization. The enriched KEGG pathways of *JUN* included pathways involved in autoimmune thyroid disease and cell adhesion molecule cascades (Fig. S1A). In terms of GO functions, CDKN1A was found to be enriched in the collagen catabolic process and is a positive regulator of autophagy. The enriched KEGG pathways of CDKN1A included pathways involved in acute myeloid leukemia and autoimmune thyroid disease (Fig. S1B). DDIT3 was found to be associated with chromosomal segregation and mitotic nuclear division (GO functions), with KEGG pathways such as those involved in autoimmune thyroid disease and cell adhesion molecule cascades (Fig. S1C). *DDIT4* was associated with GO functions such as chromosome segregation and external encapsulating structure organization and KEGG pathways such as those involved in acute myeloid leukemia and the adipocytokine signaling (Fig. S1D). *HMGB2* was enriched in GO functions such as humoral immune response and positive regulation of autophagy and KEGG pathways such as autoimmune thyroid disease and cell adhesion molecule cascades (Fig. S1E). The complete enrichment results are provided in Table S5.

Based on these features, a nomogram was constructed for OA (Fig. 5A). The ROC value in the correction curve was 1 (Fig. 5B), and the net benefit of the nomogram was the highest in the DCA curve (Fig. 5C). In terms of the clinical impact curve, the curve of the high-risk number was near the curve of the high risk with event number (Fig. 5D). In addition, the expression of the featured genes was observed in the 6 cell types identified previously. Notably, the percentages of HomC, RegC, and HTC were higher in the control samples, and the level of HomC between OA and control samples was significantly different. These differences might reflect reduced tissue repair and regenerative capacity, changes in the immune response, and altered joint stability, and further research remains necessary. (Fig. 5E) (Table 1). *CDKN1A, DDIT3,* and *JUN* were found to be highly expressed in these cells, and they were closely related to functions in cell cycle regulation, stress response and transcription factor activity. The high expression of these genes reflected cellular activities and functions, and in-depth studies could help to understand cell type characteristics and related biological processes. (Fig. 5F).

3.5. Six potential drugs that strongly bind with the featured genes

A total of 84 potential drugs targeting the featured genes were predicted, and a drug-gene network was constructed based on them (Fig. S2). Molecular docking revealed that six drugs could strongly bind with the featured genes. Of these drugs, Taxotere displayed the highest binding affinity for DDIT3 **(Table 2)**. The detailed docking results are shown in Fig. S3. These results demonstrated the varying degrees of interaction between different genes and drugs. The CDKN1A exhibited a strong interaction with the DIAZIQUONE drug, with an affinity of −4.8 kcal/mol and the formation of a hydrogen bond. Conversely, the interaction between the CDKN1A and the PENTETIC ACID drug is weaker, with an affinity of −4.1 kcal/mol and no hydrogen bond formation observed. The DDIT3 displayed a strong interaction with the TAXOTERE and CELECOXIB drugs, with affinities of −7.7 kcal/mol and −5.8 kcal/mol, respectively. However, no hydrogen bonds were formed in either case. Similarly, the JUN exhibits a relatively weaker interaction with the CHEMBL477052 and BRUCEANTIN drugs, with affinities of −4.2 kcal/mol and −5.6 kcal/mol, respectively, and no hydrogen bonds were formed in these interactions as well.

3.6. CDKN1A is essential for chondrocyte differentiation

To explore the five characteristic genes, we verified their transcription levels, levels in tissue samples, and protein expression levels. RT−qPCR revealed that *CDKN1A* and *JUN* were significantly downregulated in IL-1β-treated OA chondrocytes (OA group) compared to control cells, and *CDKN1A* was more notably downregulated than *JUN* ($p < 0.01$). However, no significant differences were found in the expression of *DDIT3*, *DDIT4*, or *HMGB2,* which indicated that the expression levels of these genes were relatively stable and not affected under the condition of IL-1β-treated OA chondrocytes. However, further in-depth investigation was needed to explore their specific expression in cartilage tissue of OA patients. (Fig. 6A).

Safranin O and immunohistochemical staining of CDKN1A and JUN were performed on knee cartilage obtained from the control and OA groups. Based on the results, the expression level of CDKN1A in the OA group was remarkably lower than that in the control group ($p < 0.01$). Intriguingly, there was no significant difference in JUN expression between the two groups (Fig. 6B and C).

The expression levels of CDKN1A and JUN were further evaluated using western blotting. The Western blot results were consistent with those of immunohistochemical staining. The expression level of CDKN1A was significantly lower in the OA group than in the control group ($p < 0.01$). However, there was no discernible variation in JUN expression (Fig. 6D and E).

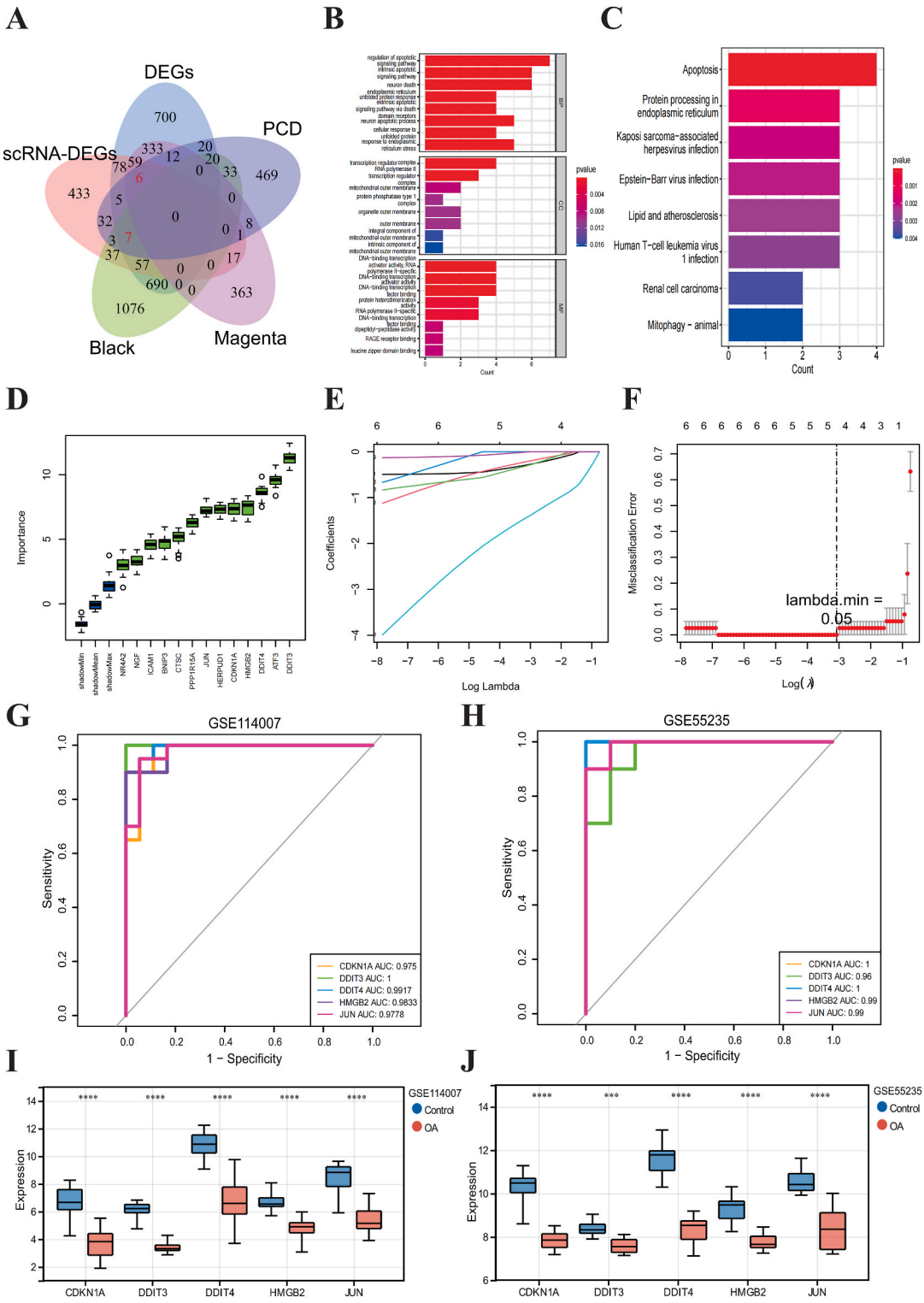

Fig. 4. Detection and verification of DEGs between OA and control samples in the merged dataset and multiple machine learning algorithm filtering of DEGs. (A) Venn diagram of the 13 overlapping genes based on the intersection of DEGs, scRNA-DEGs, key module (black, magenta) genes, and programmed PCD-related genes. (B) Gene ontology (GO) analysis of candidate genes. BP: biological process; MF: molecular functions; CC: cellular components. (C) KEGG analysis of candidate genes. (D) Identification of characteristic genes using the Boruta algorithm. The blue box plots correspond to the minimum, average, and maximum scores of a shaded attribute. The red, yellow, and green box plots represent the rejected, tentative, and confirmed scoring attributes, respectively, with green representing the significant featured gene. (E) Gene coefficient map of

characteristic genes screened via LASSO regression analysis. The abscissa represents log (Lambda) and the ordinate represents the local likelihood deviation. (F) Error graph for the cross-validation of characteristic genes screened via LASSO regression analysis. The abscissa represents log (Lambda) and the ordinate represents the coefficient of the gene. (G) ROC curve of the featured genes in GSE114007. (H) ROC curve of the featured genes in GSE55235. (I) Expression of the featured genes in GSE114007. (J) Expression of the featured genes in GSE55235. (For interpretation of the references to color in this figure legend, the reader is referred to the Web version of this article.)

To further determine whether CDKN1A plays a critical role in chondrocyte differentiation, C28/I2 human chondrocytes were micromass-cultured, and alcian blue staining was performed at different time points. Compared to the control group, s CDKN1A knockout group exhibited substantially weakened chondrocyte differentiation in a time-dependent manner (Fig. 6F and G).

We measured the expression levels of chondrocyte metabolic marker genes using RT−qPCR. After CDKN1A knockout, the expression levels of *COL2A1* and *ACAN* were significantly decreased, whereas those of *MMP-13* and *ADAMTS-5* were notably increased. Overall, CDKN1A was identified as the most characteristic DEG between the OA and control groups, and loss of CDKN1A disrupted chondrocyte differentiation (Fig. **6H)**.

4. Discussion

Cartilage loss mediated by chondrocyte death is a key mechanism in the pathogenesis of OA [11]. PCD is a death process that is regulated and triggered by the cells themselves and maintains the normal function and homeostasis of tissues and organisms by removing damaged or unwanted cells. Five main chondrocyte death pathways are associated with OA: apoptosis, necrosis, pyroptosis, ferroptosis, and autophagy [12]. These PCD pathways are functionally crosslinked and interact with each other during OA development [24]. Therefore, identifying PCD-related markers in chondrocytes is of great importance for the diagnosis and treatment of OA. In this study, we revealed the role of PCD-related genes in osteoarthritic chondrocytes using single-cell and transcriptome analyses. Six chondrocyte subtypes (HomC, HTC, RepC, preFC, FC, and RegC) were annotated via scRNA analysis, 13 candidate genes were identified using WGCNA, and five featured genes (*JUN, CDKN1A, HMGB2, DDIT3*, and *DDIT4*) were screened out using 2 machine learning algorithms. Functional analysis revealed that CDKN1A was highly involved in collagen breakdown and played a supportive role in promoting autophagy. Subsequently, the down-regulation of CDKN1A was confirmed in both joint tissues of an OA mouse model and OA model cell. By inhibiting the expression of CDKN1A, the differentiation of OA chondrocytes can be effectively suppressed.

As a founding member of the cyclin-dependent kinase (Cdk) inhibitor family, CDKN1A is involved in a variety of biological functions, such as cell cycle regulation, cell apoptosis, differentiation, migration, aging, and the initiation of cell death [25,26]. CDKN1A knockout OA model mice are prone to modifications, such as elevated osteoclast invasion and MMP expression levels [27]. In our study, CDKN1A was found to be significantly downregulated in the OA model *in vitro and in vivo.* CDKN1A had a significant inhibitory effect on chondrocyte differentiation. Our findings, together with those of previous studies, imply that CDKN1A is a potential therapeutic target for the treatment of OA.

JUN is one of the most critical mitogen-activated protein kinases (MAPKs) that regulates diverse biological processes, such as cell proliferation, differentiation, death, and survival in response to cellular stress [28,29]. JUN mediates metalloproteinase expression and joint destruction in joint arthritis [30]. JUN overexpression is also closely related to the deficiency of SOX9 transcriptional activity and suppression of COL2A1 expression in chondrocytes [31]. In this study, JUN was found to be markedly downregulated in OA chondrocytes, which is inconsistent with the results of previous studies. As members of the C/EBP family, both DDIT3 and DDIT4 are stimulated by endoplasmic reticulum stress [32,33] and are involved in cell apoptosis [34,35]. DDIT3 is highly expressed in the cartilage plate and inhibits chondrocyte differentiation by promoting SIRT1 [36]. DDIT3 deficiency enhances the chondrogenic potential of mouse ATDC5 cells [37]. In contrast, DDIT4 is a crucial modulator of articular cartilage homeostasis that positively mediates autophagy in an mTOR-independent manner. DDIT4 downregulation escalates chondrocyte death and OA progression [38]. HMGB2 exhibits a positive effect on chondrocyte proliferation and maintenance of tissue function in OA [39,40]. As a result, HMGB2 knockout mice display a typical phenotype of aging-related OA. HMGB2 regulates chondrocyte hypertrophy by targeting the RUNX2 and Wnt signaling pathways. In this study, the downregulation of DDIT4 and HMGB2 expression in OA was consistent with the results of previous studies. However, the downregulation of JUN and DDIT3 was inconsistent with the findings of previous studies. The expression levels of DDIT3, DDIT4, and HMGB2 did not significantly differ between OA and control chondrocytes.

Only a few accurate and effective treatments are available for detecting symptoms that do not appear in early OA [41]. In this study, we constructed a nomogram based on the featured genes and validated its diagnostic prediction performance, providing an early diagnostic method for the treatment of early OA that could ultimately prevent further progression and the occurrence of complications. To explore the potential molecular mechanisms associated with CDKN1A, single-gene GSEA was performed. CDKN1A was found to be positively associated with the autophagy and collagen synthesis signaling pathways and negatively associated with collagen catabolism. Studies have shown that CDKN1A maintains normal cell function by regulating autophagy [42,43]. Defective autophagy has been reported to be closely associated with chondrocyte death; autophagy is activated in normal cartilage, whereas defective autophagy leads to chondrocyte death and structural damage to the cartilage [44]. The expression levels of the autophagy markers ULK-1, Beclin-1, and LC3 are significantly lower in OA chondrocytes than in normal chondrocytes, and the maintenance of autophagic activity facilitates the survival and function of chondrocytes [45]. CDKN1A is essential for the early stages of chondrogenesis. The down-regulation of CDKN1A expression is accompanied by delayed chondrocyte differentiation, which manifests as decreased proteoglycan synthesis and matrix protein expression [46]. Single-cell pseudotime trajectory analysis revealed that the HomC chondrocyte subtype

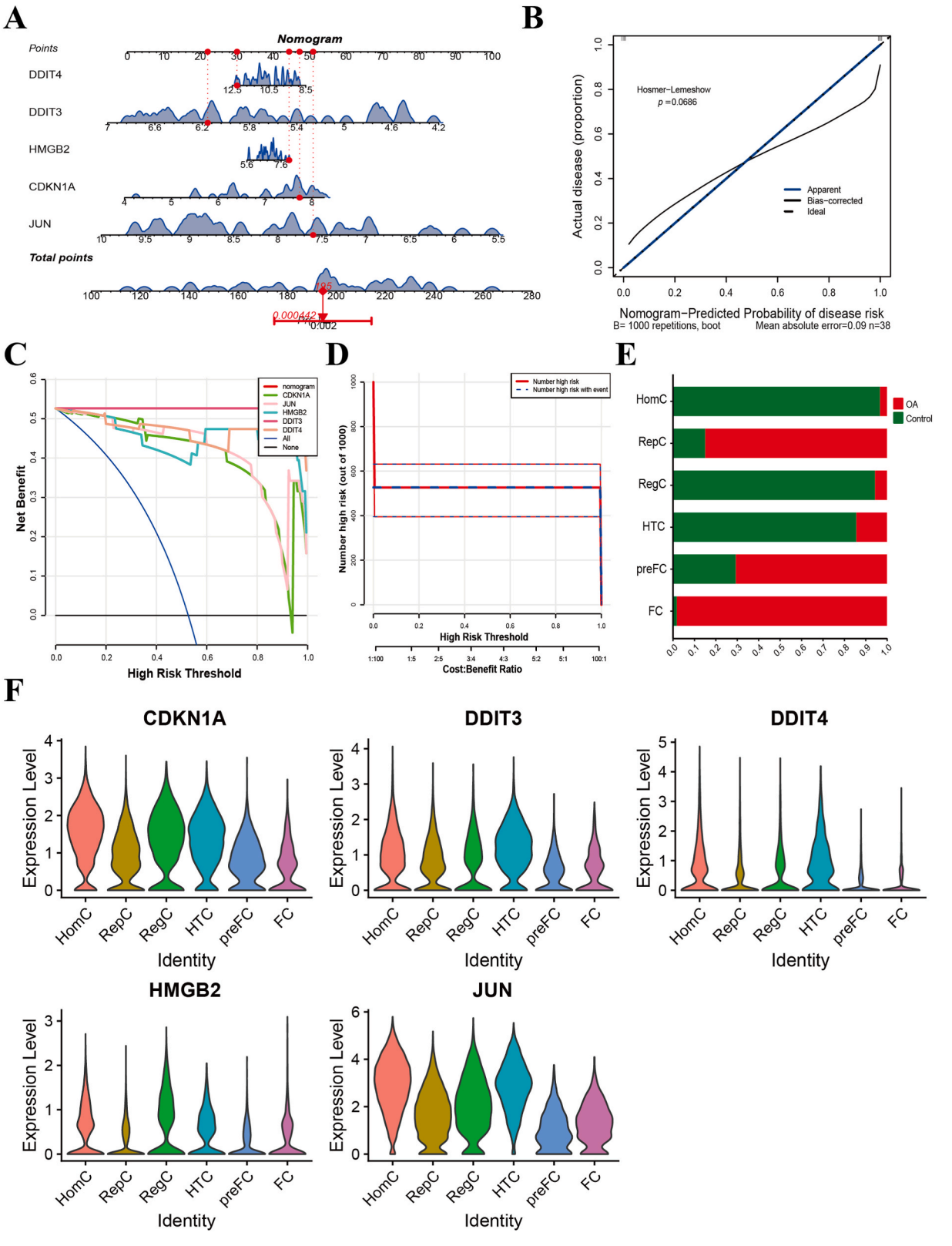

(caption on next page)

Fig. 5. Clinical evaluation of biomarkers and analysis of their expression in different chondrocyte subsets. (A) Nomogram of the featured genes (*JUN, CDKN1A, HMGB2, DDIT3*, and *DDIT4*), Nomogram was composed of "Points", "featured genes", "Total points", and "Risk of death". The x-axis represents the score for the featured genes and the y-axis represents the probability or risk of the predicted outcome. (B) ROC value in the correction curve. (C) Decision curve based on nomogram. (D) Clinical impact curve based on nomograms. (E) Percentage of different chondrocyte subtypes in OA vs. control samples. (F) Expression of the featured genes in different chondrocyte subtypes.

Table 1
The difference of cell types between OA and Control samples by *t*-Test analysis.

	Groups (average ± standard deviation)		*t*	*p*
	Control ($n = 3$)	OA ($n = 3$)		
HomC	2527.67 ± 1385.15	84.67 ± 87.15	3.049	0.038*
RepC	437.67 ± 440.28	2459.33 ± 1413.81	−2.365	0.077
RegC	889.00 ± 534.10	52.67 ± 19.40	2.710	0.113
HTC	770.00 ± 653.24	128.33 ± 211.12	1.619	0.181
preFC	177.00 ± 84.64	424.33 ± 294.82	−1.397	0.235
FC	12.67 ± 3.79	639.33 ± 898.83	−1.208	0.351

Note: $*p < 0.05$.

Table 2
Molecular docking of potential drugs.

Gene	Drug	Affinity (kcal/mol)	Hydrogen bonds
CDKN1A	DIAZIQUONE	−4.8	1
CDKN1A	PENTETIC ACID	−4.1	0
DDIT3	TAXOTERE	−7.7	0
DDIT3	CELECOXIB	−5.8	0
JUN	CHEMBL477052	−4.2	0
JUN	BRUCEANTIN	−5.6	0

was mainly present at an early stage of chondrocyte development, and CDKN1A was most clearly enriched in the HomC subtype. Therefore, we hypothesized that CDKN1A regulates chondrocyte differentiation and antagonizes chondrocyte death by regulating the autophagic pathway of the HomC subtype and cartilage collagen synthesis, thereby blocking OA progression.

The DGIdb database was used to predict drugs that target the featured genes in this study, and the predicted drug-featured gene interactions were analyzed to identify potential drugs for the treatment of OA. Based on the results, *CDKN1A, DDIT3*, and *JUN* possessed target drugs with high binding capacities. Notably, Celecoxib could bind to both CDKN1A and DDIT3 with strong affinity. As a selective nonsteroidal anti-inflammatory drug (NSAID), Celecoxib is known to significantly improve pain and inflammation in OA patients [47]. In the present study, Celecoxib was found to regulate chondrogenesis and affect OA by binding to chondroblast-related proteins. However, the role of Celecoxib in chondrocyte development requires further investigation. Paclitaxel simultaneously targets CDKN1A and DDIT3. Among the drug candidates, the derivative Taxotere exhibited the strongest binding affinity for DDIT3. In an *in vivo* experiment, paclitaxel-treated rats were used to establish a collagen-induced arthritis model. Articular cartilage morphology was found to be restored in paclitaxel-treated collagen-induced rats compared with naive rats [48]. Therefore, Paclitaxel and Taxotere may be used to treat cartilage loss in OA. However, a great deal of experimental validation is needed before a drug can be used in the clinic.

In this study, key PCD-related markers associated with chondrocyte death in OA were identified using multiple bioinformatics analyses based on different types of data (single-cell RNA-seq and bulk RNA-seq) and validation experiments. Thereafter, the potential molecular mechanisms and regulatory networks underlying these biomarkers were investigated. More importantly, the expression levels of the featured genes in OA chondrocyte subtypes were experimentally verified, and potential drugs targeting these genes were predicted. This study had some limitations. Additional experiments are required to determine the precise molecular mechanisms underlying the expression of these key genes. Owing to the influence of the sample size of this study, the heterogeneity of OA pathology, and the limitations of the technology, several possible key pathogenic compounds may have been missed during data analysis. Therefore, more clinical samples should be collected and analyzed to verify the clinical diagnostic and therapeutic value of these biomarkers.

Overall, our findings not only demonstrate that several PCD genes in osteoarthritic chondrocytes may play essential role in the development of OA but also highlight a novel approach for the evaluation and management of OA. In future studies, we will focus on the function of PCD-related markers in OA regulation and increase the sample size to verify the relationship between these key genes and clinical indices.

Ethics approval and consent to participate

The authors are accountable for all aspects of the work in ensuring that questions related to the accuracy or integrity of any part of the work are appropriately investigated and resolved. The study was approved by the Bioethics Committee of The First Affiliated

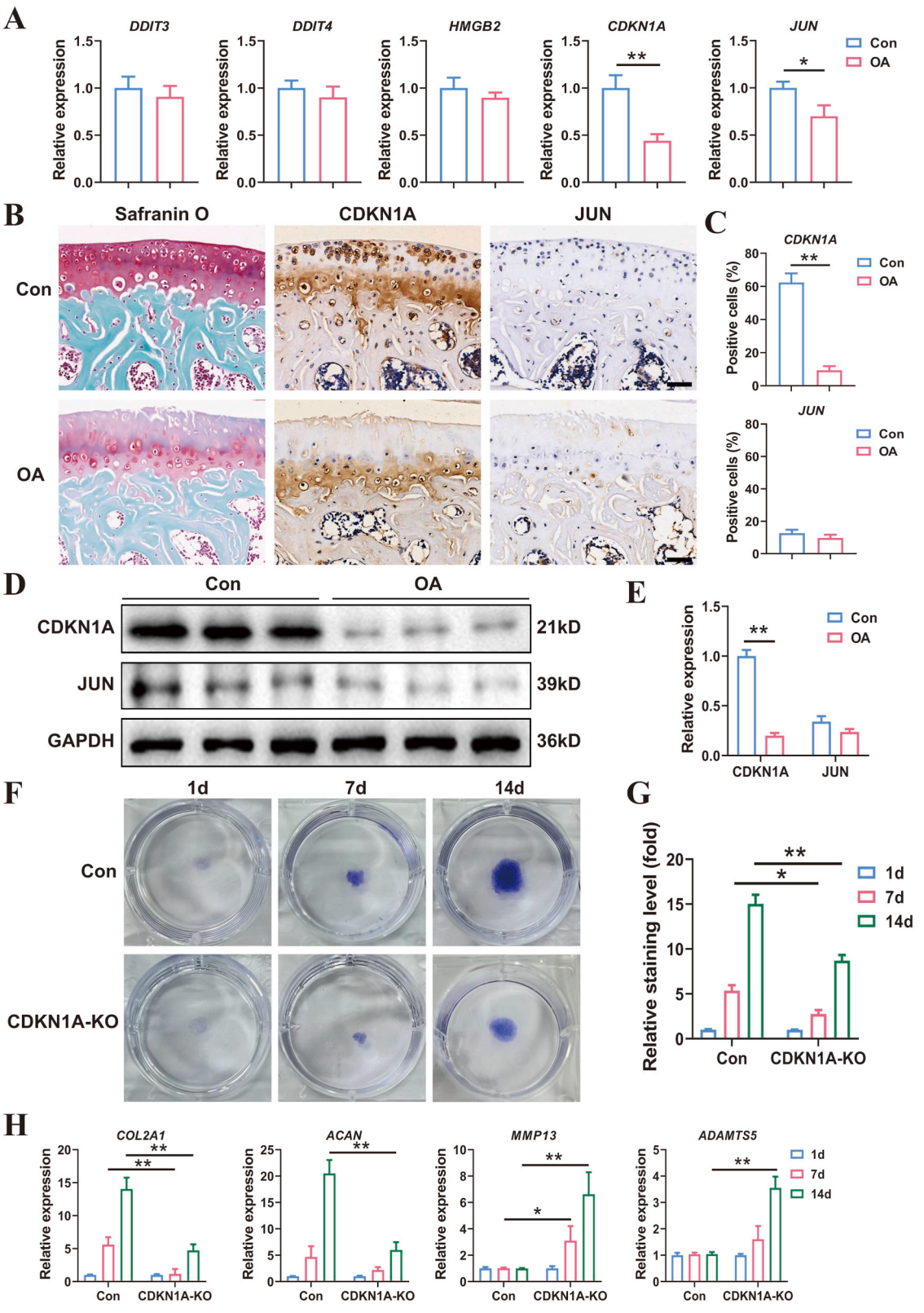

(caption on next page)

Fig. 6. Detection of CDKN1A expression and its function in chondrogenesis. (A) C28/I2 chondrocytes were incubated for 7 days, and RT-qPCR was performed to determine the expression of *JUN, CDKN1A, HMGB2, DDIT3*, and *DDIT4*. (B) Safranin O and immunohistochemical staining of CDKN1A and JUN between the control and OA groups after 8 weeks. Scale bar = 50 μm. (C) Quantitative analysis of (B). (D) Western blot assay of CDKN1A and JUN in cultured C28/I2 human chondrocytes induced for 7 days. (E) Quantitative analysis of (C). (F) Chondrogenic induction was performed in the control group and CDKN1A knockout group for 1, 7, and 14 days. Thereafter, Alcian blue staining was conducted. (G) Quantitative analysis of (F). (H) Chondrogenic induction was performed in the control group and CDKN1A knockout group for 1, 7, and 14 days. RT-qPCR was performed to examine the expression of COL2A1, ACAN, MMP-13, and ADAMTS-5. (For interpretation of the references to color in this figure legend, the reader is referred to the Web version of this article.)

Hospital of the University of Science and Technology of China No: (2023-N (A)-53).

Consent for publication

Not applicable.

Funding

This research was supported by Postdoctoral Research Foundation of China (2023M733424), Basic Medical Research Project of Changhai Hospital (2021JCQN06) and Doctoral Research Initiation Fund of the First Affiliated Hospital of the USTC (RC2021133).

Data availability statement

The RNA-seq data of human knee cartilage tissues are available in the GEO database (number GSE114007). The RNA-seq data of human knee synovial tissues are available in the GEO database (number GSE55235). The scRNA-seq data of human chondrocytes were obtained from the GEO database (number GSE152805).

CRediT authorship contribution statement

Chao Fang: Writing – review & editing, Writing – original draft, Validation, Supervision, Resources, Project administration, Methodology, Investigation, Funding acquisition, Conceptualization. **Shanbang Zhu:** Validation, Software, Methodology, Investigation, Formal analysis, Data curation, Conceptualization. **Rui Zhong:** Validation, Formal analysis, Data curation. **Gang Yu:** Validation, Methodology, Investigation. **Shuai Lu:** Validation, Software, Investigation. **Zhilin Liu:** Software, Investigation. **Jingyu Gao:** Software, Investigation. **Chengyuan Yan:** Visualization, Software, Investigation. **Yingming Wang:** Validation, Software, Investigation. **Xinzhe Feng:** Writing – review & editing, Writing – original draft, Visualization, Validation, Supervision, Resources, Project administration, Methodology, Investigation, Funding acquisition, Data curation, Conceptualization.

Declaration of competing interest

The authors declare that they have no known competing financial interests or personal relationships that could have appeared to influence the work reported in this paper.

Acknowledgements

We thank Enago for English language editing.

Abbreviations

OA	osteoarthritis
PCD	Programmed cell death
GEO	Gene Expression Omnibus
DEGs	Differentially expressed genes
WGCNA	Weighted gene co-expression network analysis
RT-qPCR	Real-Time Quantitative Polymerase Chain Reaction
WB	western blot
IHC	immunohistochemistry
PCA	Principal component analysis
t-SNE	T-distributed stochastic neighbor embedding
LASSO	Least absolute shrinkage and selection operator
scRNA-seq	Single-cell RNA sequencing
CDKN1A	cyclin-dependent kinase inhibitor-1A
PCs	principal components

GO	Gene ontology
KEGG	Kyoto encyclopedia of genes and genomes
ROC	Receiver operating characteristic
GSEA	Gene set enrichment analysis
DMEM	Dulbecco's modified Eagle's medium
FBS	fetal bovine serum
IL-1β	interleukin-1β
HDR	homology-directed repair
DMM	medial meniscus
AUC	area under the curve
MAPKs	mitogen-activated protein kinases
Cdk	cyclin-dependent kinase
NSAID	non-steroidal anti-inflammatory drug

Appendix A. Supplementary data

Supplementary data to this article can be found online at https://doi.org/10.1016/j.heliyon.2024.e27466.

References

[1] Bierma-Zeinstra Hunter, Osteoarthritis. Lancet. 393 (2019) 1745–1759, https://doi.org/10.1016/S0140-6736(19)30417-9.
[2] Cicuttini Martel-Pelletier, Barr, et al., Osteoarthritis. Nature reviews. Disease primers. 2 (2016) 16072, https://doi.org/10.1038/nrdp.2016.72.
[3] Goldring Goldring, Changes in the osteochondral unit during osteoarthritis: structure, function and cartilage-bone crosstalk, Nat. Rev. Rheumatol. 12 (2016) 632–644, https://doi.org/10.1038/nrrheum.2016.148.
[4] Arant Katz, Loeser, diagnosis and treatment of hip and knee osteoarthritis: a review, JAMA 325 (2021) 568–578, https://doi.org/10.1001/jama.2020.22171.
[5] da Costa, Keller Reichenbach, et al., Effectiveness of non-steroidal anti-inflammatory drugs for the treatment of pain in knee and hip osteoarthritis: a network meta-analysis, Lancet 390 (2017) e21–e33, https://doi.org/10.1016/S0140-6736(17)31744-0.
[6] Price, Alvand, Troelsen, et al., Knee replacement, Lancet 392 (2018) 1672–1682, https://doi.org/10.1016/S0140-6736(18)32344-4.
[7] L. Foster, L, et al., Osteoarthritis Year in Review 2022: Epidemiology & Therapy. Osteoarthritis and Cartilage, 2023, https://doi.org/10.1016/j.joca.2023.03.008.
[8] Lorenzo, Bayliss, Heinegard, Altered patterns and synthesis of extracellular matrix macromolecules in early osteoarthritis, Matrix Biol. : journal of the International Society for Matrix Biology 23 (2004) 381–391, https://doi.org/10.1016/j.matbio.2004.07.007.
[9] Matisic Molnar, Kodvanj, et al., Cytokines and Chemokines involved in osteoarthritis pathogenesis, Int. J. Mol. Sci. 22 (2021), https://doi.org/10.3390/ijms22179208.
[10] Beier Pitsillides, Cartilage biology in osteoarthritis–lessons from developmental biology, Nat. Rev. Rheumatol. 7 (2011) 654–663, https://doi.org/10.1038/nrrheum.2011.129.
[11] Green, The coming decade of cell death research: five riddles, Cell 177 (2019) 1094–1107, https://doi.org/10.1016/j.cell.2019.04.024.
[12] Yang, Bian Hu, et al., Targeting cell death: pyroptosis, ferroptosis, apoptosis and necroptosis in osteoarthritis, Front. Cell Dev. Biol. 9 (2021) 789948, https://doi.org/10.3389/fcell.2021.789948.
[13] Kolodziejczyk, Kim, Svensson, et al., The technology and biology of single-cell RNA sequencing, Mol. Cell 58 (2015) 610–620, https://doi.org/10.1016/j.molcel.2015.04.005.
[14] Saliba, Westermann, Gorski, et al., Single-cell RNA-seq: advances and future challenges, Nucleic Acids Res. 42 (2014) 8845–8860, https://doi.org/10.1093/nar/gku555.
[15] Murphy Ito, Application of ggplot2 to pharmacometric graphics, CPT Pharmacometrics Syst. Pharmacol. 2 (2013) e79, https://doi.org/10.1038/psp.2013.56.
[16] Jain Chou, Gibson, et al., Synovial cell cross-talk with cartilage plays a major role in the pathogenesis of osteoarthritis, Sci. Rep. 10 (2020) 10868, https://doi.org/10.1038/s41598-020-67730-y.
[17] Phipson Ritchie, Wu, et al., Limma powers differential expression analyses for RNA-sequencing and microarray studies, Nucleic Acids Res. 43 (2015) e47, https://doi.org/10.1093/nar/gkv007.
[18] Horvath Langfelder, WGCNA: an R package for weighted correlation network analysis, BMC Bioinf. 9 (2008) 559, https://doi.org/10.1186/1471-2105-9-559.
[19] Wu, Xu Hu, et al., clusterProfiler 4.0: a universal enrichment tool for interpreting omics data, Innovation 2 (2021) 100141, https://doi.org/10.1016/j.xinn.2021.100141.
[20] Sherwood, Nalesso Bertrand, et al., A homeostatic function of CXCR2 signalling in articular cartilage, Ann. Rheum. Dis. 74 (2015) 2207–2215, https://doi.org/10.1136/annrheumdis-2014-205546.
[21] Nalesso, Sherwood, Bertrand, et al., WNT-3A modulates articular chondrocyte phenotype by activating both canonical and noncanonical pathways, J. Cell Biol. 193 (2011) 551–564, https://doi.org/10.1083/jcb.201011051.
[22] De Bari Eltawil, Achan, et al., A novel in vivo murine model of cartilage regeneration. Age and strain-dependent outcome after joint surface injury, Osteoarthritis Cartilage 17 (2009) 695–704, https://doi.org/10.1016/j.joca.2008.11.003.
[23] Crane Cui, Xie, et al., Halofuginone attenuates osteoarthritis by inhibition of TGF-beta activity and H-type vessel formation in subchondral bone, Ann. Rheum. Dis. 75 (2016) 1714–1721, https://doi.org/10.1136/annrheumdis-2015-207923.
[24] Xu Tang, Zhang, et al., Ferroptosis, necroptosis, and pyroptosis in anticancer immunity, J. Hematol. Oncol. 13 (2020) 110, https://doi.org/10.1186/s13045-020-00946-7.
[25] Kreis, Louwen, Yuan, Less understood issues: p21(Cip1) in mitosis and its therapeutic potential, Oncogene 34 (2015) 1758–1767, https://doi.org/10.1038/onc.2014.133.
[26] Dutta Abbas, p21 in cancer: intricate networks and multiple activities, Nat. Rev. Cancer 9 (2009) 400–414, https://doi.org/10.1038/nrc2657.
[27] Kihara, Hayashi, Hashimoto, et al., Cyclin-dependent kinase inhibitor-1-deficient mice are susceptible to osteoarthritis associated with enhanced inflammation, J. Bone Miner. Res. : the official journal of the American Society for Bone and Mineral Research 33 (2018) 2242, https://doi.org/10.1002/jbmr.3613.
[28] Pua, Chung Mai, et al., Functional roles of JNK and p38 MAPK signaling in nasopharyngeal carcinoma, Int. J. Mol. Sci. 23 (2022), https://doi.org/10.3390/ijms23031108.
[29] Chen, Wan Ye, et al., The roles of c-jun N-terminal kinase (JNK) in infectious diseases, Int. J. Mol. Sci. 22 (2021), https://doi.org/10.3390/ijms22179640.

[30] Boyle Han, Chang, et al., c-Jun N-terminal kinase is required for metalloproteinase expression and joint destruction in inflammatory arthritis, J. Clin. Invest. 108 (2001) 73–81, https://doi.org/10.1172/JCI12466.
[31] Yu Hwang, Poo, et al., c-Jun/activator protein-1 mediates interleukin-1beta-induced dedifferentiation but not cyclooxygenase-2 expression in articular chondrocytes, J. Biol. Chem. 280 (2005) 29780–29787, https://doi.org/10.1074/jbc.M411793200.
[32] Pina, Teles, Fugazza, et al., Single-cell network analysis identifies DDIT3 as a nodal lineage regulator in hematopoiesis, Cell Rep. 11 (2015) 1503–1510, https://doi.org/10.1016/j.celrep.2015.05.016.
[33] Sinks Deng, Elliot, et al., Characterisation of respiratory health and exposures at a sintered permanent magnet manufacturer, Br. J. Ind. Med. 48 (1991) 609–615, https://doi.org/10.1136/oem.48.9.609.
[34] ToddLee Glimcher, The endoplasmic reticulum stress response in immunity and autoimmunity, Nat. Rev. Immunol. 8 (2008) 663–674, https://doi.org/10.1038/nri2359.
[35] Shoshani, Faerman, Mett, et al., Identification of a novel hypoxia-inducible factor 1-responsive gene, RTP801, involved in apoptosis, Mol. Cell Biol. 22 (2002) 2283–2293, https://doi.org/10.1128/MCB.22.7.2283-2293.2002.
[36] Xu Yu, Dong, et al., DDIT3/CHOP mediates the inhibitory effect of ER stress on chondrocyte differentiation by AMPKalpha-SIRT1 pathway, Biochim. Biophys. Acta Mol. Cell Res. 1869 (2022) 119265, https://doi.org/10.1016/j.bbamcr.2022.119265.
[37] Yu, Wu Yi, et al., Ddit3 suppresses the differentiation of mouse chondroprogenitor cells, Int. J. Biochem. Cell Biol. 81 (2016) 156–163, https://doi.org/10.1016/j.biocel.2016.11.009.
[38] Alvarez-Garcia, Olmer Matsuzaki, et al., Regulated in development and DNA damage response 1 deficiency impairs autophagy and mitochondrial biogenesis in articular cartilage and increases the severity of experimental osteoarthritis, Arthritis Rheumatol. 69 (2017) 1418–1428, https://doi.org/10.1002/art.40104.
[39] Liu, Zhou He, et al., HMGB2 promotes chondrocyte proliferation under negative pressure through the phosphorylation of AKT, Biochim. Biophys. Acta Mol. Cell Res. 1868 (2021) 119115, https://doi.org/10.1016/j.bbamcr.2021.119115.
[40] Zhou, Deng Lu, et al., HMGB2 is associated with pressure loading in chondrocytes of temporomandibular joint: in vitro and in vivo study, Cytokine 126 (2020) 154875, https://doi.org/10.1016/j.cyto.2019.154875.
[41] Camacho-Encina, Balboa-Barreiro, Rego-Perez, et al., Discovery of an autoantibody signature for the early diagnosis of knee osteoarthritis: data from the Osteoarthritis Initiative, Ann. Rheum. Dis. 78 (2019) 1699–1705, https://doi.org/10.1136/annrheumdis-2019-215325.
[42] Xu, Wan, Huang, et al., Oridonin protects against cardiac hypertrophy by promoting P21-related autophagy, Cell Death Dis. 10 (2019) 403, https://doi.org/10.1038/s41419-019-1617-y.
[43] Huang, Xu, Liu, et al., Autophagy is involved in the protective effect of p21 on LPS-induced cardiac dysfunction. Cell Death Dis.. 11 (2020) 554, https://doi.org/10.1038/s41419-020-02765-7..
[44] Carames, Olmer, Kiosses, et al., The relationship of autophagy defects to cartilage damage during joint aging in a mouse model. Arthritis Rheumatol.. 67 (2015) 1568-1576, https://doi.org/10.1002/art.39073..
[45] Im Jeon, Autophagy in osteoarthritis, Connect. Tissue Res. 58 (2017) 497–508, https://doi.org/10.1080/03008207.2016.1240790.
[46] Simsa-Maziel, Monsonego-Ornan, Interleukin-1beta promotes proliferation and inhibits differentiation of chondrocytes through a mechanism involving down-regulation of FGFR-3 and p21, Endocrinology 153 (2012) 2296–2310, https://doi.org/10.1210/en.2011-1756.
[47] Goa Clemett, Celecoxib: a review of its use in osteoarthritis, rheumatoid arthritis and acute pain, Drugs 59 (2000) 957–980, https://doi.org/10.2165/00003495-200059040-00017.
[48] Arsenault, Lhotak, Hunter, et al., Taxol (paclitaxel) involution of articular cartilage destruction in collagen induced arthritis: an ultrastructural demonstration of an increased superficial chondroprotective layer, J. Rheumatol. 27 (2000) 582–588.